

Spin Dynamics in $S = 1/2$ Chains with Next-Nearest-Neighbor Exchange Interactions

M. Ozerov,¹ E. Čížmár,^{1,2} J. Wosnitza,¹ S.A. Zvyagin,¹ A.A. Zvyagin,^{3,4} R. Feyerherm,⁵ F. Xiao,⁶ and C.P. Landee⁶

¹Dresden High Magnetic Field Laboratory (HLD),

Forschungszentrum Dresden-Rossendorf (FZD), 01314 Dresden, Germany

²Centre of Low Temperature Physics, P.J. Šafárik University, SK-041 54 Košice, Slovakia

³Institut für Festkörperphysik, Technische Universität Dresden, 01069 Dresden, Germany

⁴B. Verkin Institute for Low Temperature Physics and Engineering,
National Academy of Science of Ukraine, Kharkov, 61103, Ukraine

⁵Helmholtz-Zentrum Berlin (HZB) für Materialien und Energie GmbH, 12489 Berlin, Germany

⁶Department of Physics and Carlson School of Chemistry, Clark University, Worcester, MA 01060, USA

(Dated: April 15, 2010)

Low energy magnetic excitations in the spin-1/2 chain compound (6MAP)CuCl₃ are probed by means of tunable-frequency electron spin resonance (ESR). Two modes with asymmetric (with respect to the $h\nu = g\mu_B B$ line) frequency-field dependences are resolved, illuminating the strike incompatibility with a simple uniform $S = \frac{1}{2}$ Heisenberg chain model. The unusual ESR spectrum is explained in terms of the recently developed theory for spin-1/2 chains, suggesting the important role of next-nearest-neighbor interactions in this compound. Our conclusion is supported by model calculations for the magnetic susceptibility of (6MAP)CuCl₃, revealing a good qualitative agreement with experiment.

PACS numbers: 75.40.Gb, 76.30.-v, 75.10.Jm

Introduction.— A spin-1/2 Heisenberg antiferromagnetic (AF) chain is one of paradigms in modern quantum many-body physics. The most important feature of this model is its integrability by means of the famous Bethe ansatz¹. However, as revealed theoretically and experimentally, the uniform spin chains are unstable with respect to any perturbation, breaking the chain uniformity. Such instability gives rise to a rich variety of strongly correlated spin states and quantum phase transitions, making these objects an attractive ground for testing various theoretical concepts experimentally. A competition between nearest-neighbor (NN) and next-nearest-neighbor (NNN) interactions, as well as the presence of magnetic anisotropy, can fundamentally modify the ground-state properties of quantum spin chains resulting in a large diversity of complex magnetic structures^{2–6}. The experimental determination of these interactions often is a challenging task. For that, magnetic and thermodynamic measurements (magnetization, magnetic susceptibility, specific heat) can be regarded as a very initial tool, providing very often only the overall and not sufficient detailed picture of magnetic interactions in low-dimensional spin systems. Inelastic neutron scattering, on the other hand, is a more suitable tool, but it has certain serious limitations (including, for instance, requirements on the sample size and chemical composition of the material). That is why, the search for new approaches (both theoretical and experimental) that are helpful in clarifying the microscopic structure of magnetic interactions appears to be of particular importance.

Electron spin resonance (ESR) is traditionally recognized as one of the most sensitive techniques for probing magnetic excitations in spin systems with collective ground states (see for instance Refs. 7–10). Here, we present ESR studies of the low-energy excitation spec-

trum in the $S = \frac{1}{2}$ chain system (C₆H₉N₂)CuCl₃ (hereafter (6MAP)CuCl₃). Two gapped modes with asymmetric (with respect to the $h\nu = g\mu_B B$ line) resonance positions have been observed in the low-temperature ESR spectrum, reflecting the discrepancy with the simple spin-1/2 Heisenberg AF chain model, employed for this compound previously¹¹. Our data are interpreted in the frame of the recently developed mean-field-like theory for spin-1/2 chains¹², strongly suggesting the elementary magnetic cell multiplication and presence of NNN interactions in this compound.

Experimental and discussion.— (6MAP)CuCl₃ crystallizes in the orthorhombic structure belonging to the space group $Pnma$, with lattice constants $a = 11.4$ Å, $b = 6.6$ Å, $c = 12.8$ Å (determined at room temperature), and number of formula units per unit cell $Z = 4$ ¹¹.

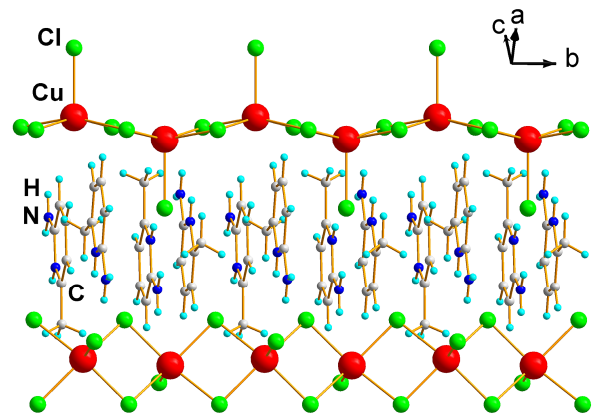


FIG. 1: (Color online) Crystal structure of (6MAP)CuCl₃.

The compound is built up from well-isolated, doubly bridged linear chains of Cu^{2+} ions (Fig. 1). There are two types of crystallographically similar chains running along the b axis. Each copper ion has a square-pyramidal coordination geometry, with the axial bond substantially longer than the basal ones, and with the direction of the axial bond alternating along the chain axis b . The Cu-Cl-Cu bridging angle is well above 90° , which defines the AF nature of the NN exchange interactions ($J/k_B \approx 110$ K^{11,13}). Using the formula for the Néel temperature T_N from Ref. 14 and assuming $T_N < 100$ mK (as evident from muon spin relaxation experiments¹⁵), the interchain interaction J'/k_B is estimated to be less than 40 mK, suggesting $J'/J < 4 \cdot 10^{-4}$ and indicating almost perfect one-dimensional nature of magnetic correlations in (6MAP)CuCl₃. However, below about 15 K a deviation from the expected for a spin-1/2 uniform Heisenberg AF chain behavior appears^{11,13,16}, i.e., the low-temperature magnetic susceptibility shows a pronounced low-temperature upturn. Very often, in spin-chain compounds such a low-temperature tail in magnetic susceptibility originates from the broken-chain effects and/or defects, overshadowing the intrinsic low-temperature susceptibility behavior (which is of particular importance when describing the ground state of spin chain materials). To get a deeper insight into the ground state nature in (6MAP)CuCl₃ we decided to probe the low-temperature excitation spectrum in this compound by use of ESR measurements.

ESR experiments have been performed at the Dresden High Magnetic Field Laboratory (Hochfeld Magnetlabor Dresden, HLD) using an X-band spectrometer (Bruker ELEXSYS E500) at a fixed frequency of 9.4 GHz and a tunable-frequency ESR spectrometer (similar to that described in Ref. 17). High-quality single-crystalline (6MAP)CuCl₃ samples with a typical size of 1.5x1.5x4 mm³ were used. The magnetic field was applied along the b axis. The magnetization measurements have been performed on a standard "Quantum Design" PPMS system.

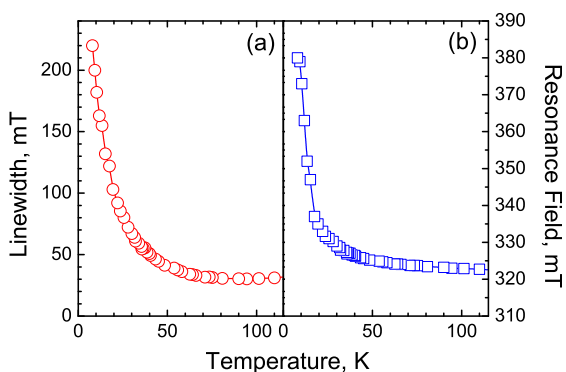


FIG. 2: (Color online) Temperature dependence of the linewidth (a) and resonance field (b) measured at a frequency of 9.4 GHz. Lines are guides to the eye.

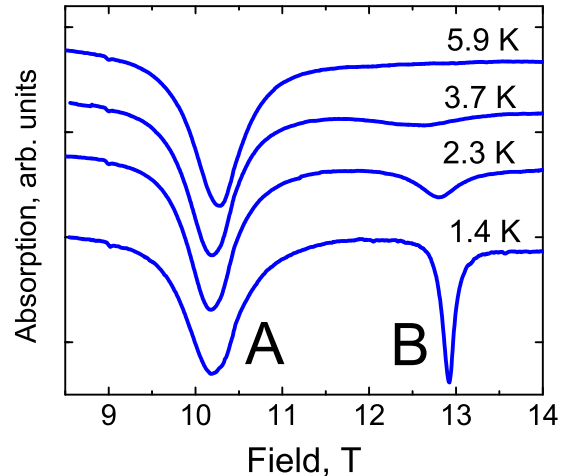


FIG. 3: (Color online) ESR spectra of (6MAP)CuCl₃ obtained at a frequency of 300 GHz for different temperatures.

A single ESR line (with $g = 2.06$ measured at 20 K) was observed at temperatures above 5 K. It was shown theoretically¹⁹, that the ESR response of an ideal uniform Heisenberg spin chain with magnetically isotropic interactions should reveal a single peak in the ESR absorption with zero linewidth¹⁸, and with the position of the resonance proportional to the applied magnetic field. Spin-spin correlations would yield a shift of the resonance position and a broadening of the ESR line *only* in the presence of the magnetic anisotropy. The temperature dependence of ESR characteristics measured at frequency 9.4 GHz down to 7 K is shown in Fig. 2, confirming unambiguously the incompatibility of the observed ESR linewidth behavior with the simple uniform $S = \frac{1}{2}$ Heisenberg chain model. Low-temperature upturn of the linewidth, seen in Fig. 2, can be explained by the presence of relevant perturbations (from the viewpoint of renormalization group) of the critical Heisenberg chain (for instance, multiplication of elementary cell, caused by the symmetric (exchange), asymmetric (Dzyaloshinskii-Moriya) spin-spin interactions, or g -tensors)¹⁹.

To study the frequency-field dependence of magnetic excitations in (6MAP)CuCl₃, further experiments were performed using high-field (up to 16 T) tunable-frequency ESR spectrometer. Below ~ 5 K a second resonance mode (the mode B, Fig. 3) appears. The frequency-field diagram of magnetic excitations in (6MAP)CuCl₃ obtained at 1.4 K is shown in Fig. 4. The resonance absorptions in the studied frequency-field range have a linear field dependence with $g \approx 2$. Linear extrapolations of the frequency-field dependencies of the ESR modes A and B to zero field yield the resonance field shifts $\Delta_A = 15.9$ GHz (0.76 K) and $\Delta_B = -59$ GHz (-2.83 K), respectively. The observation of two gapped

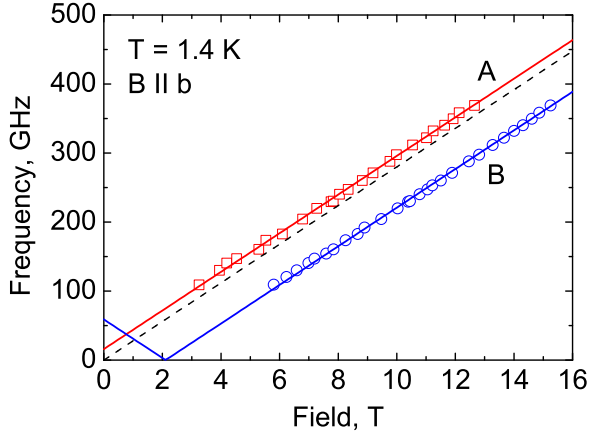


FIG. 4: (Color online) Field dependence of the magnetic-excitation frequencies in (6MAP)CuCl₃ at $T = 1.4$ K. Symbols denote experimental data, while solid lines correspond to theoretical results (see text for details). The dashed line denotes $h\nu = g\mu_B B$ for $g = 2$ (where h is the Planck constant, ν is the excitation frequency, μ_B is Bohr's magneton, and B is the magnetic field).

modes clearly indicates the incompatibility with the simple uniform magnetically isotropic spin-1/2 Heisenberg AF model, suggesting the presence of additional interactions in this compound.

Recently, the dynamical mean-field-like theory for the ESR in spin-1/2 chains with NN and NNN interactions (zigzag spin ladders) has been developed¹². It was shown that in the case of the alternation of NN interactions, ESR has to manifest itself in two resonance modes at frequencies $h\nu_{1,2} = |g\mu_B B + \Delta_{1,2}|$, where

$$\begin{aligned} \Delta_{1,2} = & \frac{1}{2} \left[(J_1 + J_2 + A_1 + A_2)R_+ \right. \\ & \pm \left((J_1 + J_2 - 2A_N)^2 R_+^2 + (A_1 + A_2 - 2A_N) \right. \\ & \left. \left. \times (2J_1 + 2J_2 - 2A_N + A_1 + A_2)R_-^2 \right)^{1/2} \right]. \quad (1) \end{aligned}$$

Here B is the value of the applied magnetic field, μ_B is the Bohr's magneton, J_1 and J_2 are the constants of spin-spin isotropic interactions along the chain, A_1 and A_2 are constants of the magnetic anisotropy, while A_N is the constant of the magnetically anisotropic NNN interaction. $R_{\pm} = \langle S_{0,1}^z \rangle \pm \langle S_{0,2}^z \rangle$ are the sum and the difference of average values of projections of magnetic moments of two magnetic centers (in the absence of the oscillating microwave field), respectively. Importantly, depending on the sign and strength of NN and NNN interactions, the theory predicts different frequency-field diagrams of magnetic excitations which can be observed using ESR. ESR experiments on the frustrated spin-1/2 quasi-one-

dimensional systems In₂VO₅²⁰, Li₂ZrCuO₄²¹, and on the asymmetric spin-ladder compound IPA-CuCl₃²² revealed qualitative agreement with the theoretical predictions.

Contrary to uniform spin-1/2 Heisenberg AF chains the combined effect of alternation and magnetic anisotropy is predicted to manifest itself in the opening of a gap in the ESR spectrum. Most importantly, the presence of the AF NN and large enough NNN interactions $[A_N[\langle S_{0,1}^z \rangle^2 + \langle S_{0,2}^z \rangle^2] > (A_1 + A_2)\langle S_{0,1}^z \rangle \langle S_{0,2}^z \rangle]$ should result in an asymmetric (with respect to the $h\nu = g\mu_B B$ line) frequency-field dependences of ESR positions (Fig. 4 in Ref. 12). This proposed frequency-field dependence is consistent with our observations in (6MAP)CuCl₃, strongly suggesting the presence of the NNN interaction and alternation in this compound.

It is important to notice that the double-mode structure of the ESR spectrum in (6MAP)CuCl₃ appears below 5 K. This temperature coincides with the activation barrier energy $E^*/k_B \approx 5$ K²³, suggesting a hydrogen position disorder in the amino groups linking the Cu chains¹¹ as an origin of the alternation²⁵.

The presence of additional interactions responsible for the energy gap opening in the low-energy ESR spectrum should manifest itself also in a peculiar behavior of magnetic susceptibility at temperatures $T \sim \Delta_{1,2}/k_B$. On the other hand, the observation of a broad maximum in the susceptibility of (6MAP)CuCl₃ at $T \sim 70$ K implies the presence of short-range-order spin correlations with the energy of the order of this temperature. Hence, additional magnetic eigenstates with energies much larger than the gaps, observed in the ESR experiments, need to be included. To describe both the magnetic susceptibility and the ESR data, a four-sublattice model can be taken as minimal. Different values of exchange couplings (defined as $\tilde{J}_{1,2,3,4}$) between the neighboring sites along the chain would yield the multiplication of the magnetic unit cell, and as consequence four ESR modes in the excitation spectrum are expected.

Since no integrable four-center Heisenberg AF spin model for (6MAP)CuCl₃ is available, the simplified four-center XY model²⁶ is applied to illustrate the proposed scenario. The exceptional usefulness of this model is determined by its exact solvability. The dispersion laws of the four excitation branches, A, B, C, and D, are shown in Fig. 5. The best agreement between the ESR data and calculations was obtained using the parameters $\tilde{J}_1/k_B = \tilde{J}_3/k_B = 105$ K, $\tilde{J}_2/k_B = 110$ K, $\tilde{J}_4/k_B = 96$ K, and $\tilde{J}_N/k_B = 0.8$ K for the alternating NN (\tilde{J}_{1-4}) and NNN (\tilde{J}_N) interactions, respectively. The theory predicts also the existence of two higher-energy ESR transitions (the mode C and D).

In Fig. 6, we show experimental data (collected at temperatures down to 1.8 K) together with the calculated (based on the four-center model) temperature dependence of the magnetic susceptibility using the obtained parameters. As follows from the model, the presence of low-energy ESR gaps observed in our experiments should determine the low- T part of the magnetic susceptibility,

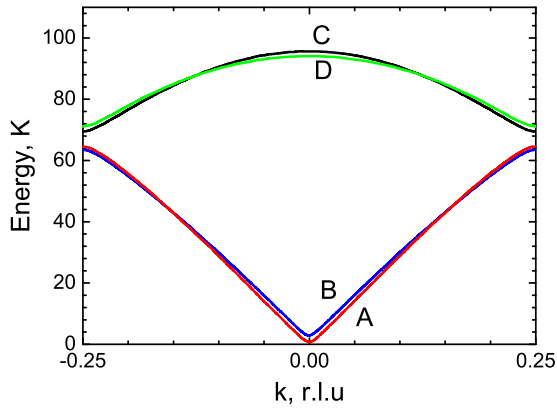


FIG. 5: (Color online) Dispersion relations of elementary excitations at $B = 0$, determined by use of a four-center spin model.

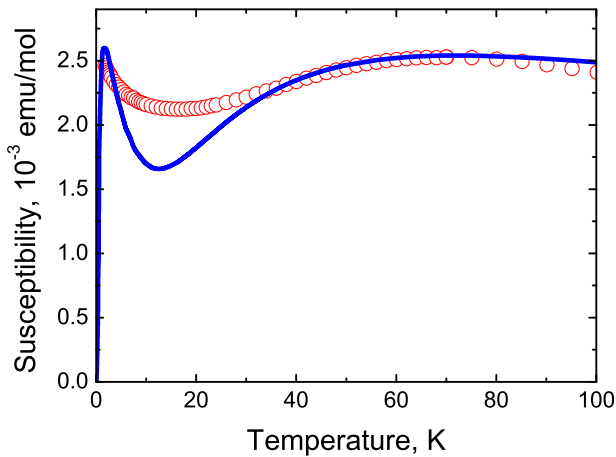


FIG. 6: (Color online) Temperature dependence of the magnetic susceptibility of $(6\text{MAP})\text{CuCl}_3$ with a magnetic field of 0.1 T applied along the b axis. Experimental data are shown by symbols, while the solid line corresponds to theoretical estimations for the four-center model with the same set of parameters as in Fig. 5 (see the text for details).

while the high-energy branches (and the related gaps) are responsible for the high- T magnetic susceptibility dependence. The main features of the calculated susceptibility behavior (low-temperature maximum, a pronounced dip at $T \approx 13$ K, and a broad maximum at $T \approx 70$ K) are consistent with the experimental data, suggesting the validity of the four-center spin-chain model with NNN interaction proposed for $(6\text{MAP})\text{CuCl}_3$. Detailed theoretical calculations of the four-center AF spin chain with NN and NNN interactions (unfortunately, not available now) is necessary to precisely determine characteristics (exchange integrals, values of the magnetic anisotropy) of the studied compound.

Conclusion. — To summarize, employing the recently developed theory for ESR in alternating spin chains the asymmetric double-peak ESR structure observed in $(6\text{MAP})\text{CuCl}_3$ is interpreted as a signature of the NNN interactions. The proposed four-center spin-chain model consistently describes both the observed ESR spectrum and the magnetic susceptibility. Hence, based on the proposed model our study has demonstrated the potential feasibility of using ESR to probe NNN interactions in alternating spin chains with high resolution (available for ESR). Our approach can be of particular importance for understanding the nature of the ground state and low-temperature magnetic properties of a wide range of spin-chain systems with competing NN and NNN exchange interactions. Our observations call for systematic neutron scattering studies of $(6\text{MAP})\text{CuCl}_3$, which would allow to verify the proposed model.

The authors would like to thank M. Turnbull and A.K. Kolezhuk for fruitful discussions. This work was partly supported by the Deutsche Forschungsgemeinschaft and EuroMagNET (EU contract No. 228043). E.C. appreciates the support by APVV-VVCE-0058-07 and APVV-0006-07. A.A.Z. appreciates the support from the Deutsche Forschungsgemeinschaft via the Mercator Program and from the Institute of Chemistry of the V.N. Karazin Kharkov National University.

¹ H.A. Bethe, Z. Phys. **71**, 205 (1931).

² See, e.g., A.A. Zvyagin *Finite Size Effects in Correlated Electron Models: Exact Results*, Imperial College Press, London (2005) and references therein.

³ P. Pincus, Solid State Commun. **9**, 1971 (1971); M.C. Cross, D.S. Fisher, Phys. Rev. B **19**, 402 (1979).

⁴ F.D.M. Haldane, Phys. Rev. B **25**, 4925 (1982); K. Okamoto and K. Nomura, Phys. Lett. A **169**, 433 (1992).

⁵ S.-L. Drechsler, O. Volkova, A.N. Vasiliev, N. Tristan, J. Richter, M. Schmitt, H. Rosner, J. Malek, R. Klingeler, A.A. Zvyagin, and B. Buchner, Phys. Rev. Lett. **98**,

077202 (2007).

⁶ C.N. Yang and C.P. Yang, Phys. Rev. **150**, 327 (1966); A.A. Zvyagin, J. Phys.: Condens. Matter **3**, 3865 (1991); A.A. Zvyagin, Zh. Eksp. Teor. Fiz. **98**, 1396 (1990).

⁷ A. K. Hassan, L.A. Pardi, G.B. Martins, G. Cao, and L-C. Brunel, Phys. Rev. Lett. **80**, 1984 (1998).

⁸ K. Katsumata, J. Phys. Cond. Matter **12**, R589 (2000).

⁹ S. Hill, R.S. Edwards, N. Aliaga-Alcalde, G. Christou, Science **302**, 1015 (2003).

¹⁰ S.A. Zvyagin, A.K. Kolezhuk, J. Krzystek, and R. Feyerherm, Phys. Rev. Lett. **93**, 027201 (2004).

¹¹ U. Geiser, R.M. Gaura, R.D. Willet, and D.X. West, Inorg.

- Chem. **25**, 4203 (1986).
- ¹² A.A. Zvyagin, Phys. Rev. B **79**, 064422 (2009).
- ¹³ Y. Liu, J.E. Drumheller, and R.D. Willett, Phys. Rev. B **52**, 15327 (1995).
- ¹⁴ C. Yasuda, S. Todo, K. Hukushima, F. Alet, M. Keller, M. Troyer, and H. Takayama, Phys. Rev. Lett. **94**, 217201 (2005).
- ¹⁵ S. Blundell *et al.*, unpublished.
- ¹⁶ M. Ozerov, E. Čížmár, J. Wosnitza, S.A. Zvyagin, F. Xiao, C.P. Landee, and M.M. Turnbull, J. Phys: Conf. Series **150** 042159 (2009).
- ¹⁷ S.A. Zvyagin, J. Krzystek, P.H.M. van Loosdrecht, G. Dhalenne, and A. Revcolevschi, Physica B **346-347**, 1 (2004).
- ¹⁸ In the absence of spin-lattice and electron-nuclear couplings, i.e., caused by the electron spin-spin interactions only.
- ¹⁹ M. Oshikawa and I. Affleck, Phys. Rev. Lett. **82**, 5136 (1999); A.A. Zvyagin, Phys. Rev. B **63**, 172409 (2001); M Oshikawa and I. Affleck, Phys. Rev. B **65**, 134410 (2002).
- ²⁰ A. Möller, T. Taetz, N. Hollmann, J.A. Mydosh, V. Kataev, M. Yehia, E. Vavilova, and B. Büchner, Phys. Rev. B **76**, 134411 (2007).
- ²¹ E. Vavilova, A.S. Moskvina, A. Arango, A. Sotnikov, S.L. Drechsler, R. Klingeler, O. Volkova, A. Vasiliev, V. Kataev, and B. Büchner, Eur. Phys. Lett. **88**, 27001 (2009).
- ²² H. Manaka and I. Yamada, Phys. Rev. B **62**, 14279 (2000).
- ²³ A pronounced maximum of a nonmagnetic origin observed at $T \approx 2.3$ K by means of specific heat¹⁶ corresponds to the activation barrier energy $E^*/k_B \approx 5$ K²⁴ and can be associated with the reported disorder.
- ²⁴ H. Kitaguchi, S. Nagata, and T. Watanabe, J. Phys. Soc. Japan **41**, 1159 (1976).
- ²⁵ Such an alternation can be caused, for instance, by different magnetic interactions along the chain as result of a spin-Peierls transition. However, a thorough search for possible superstructures by synchrotron x-ray diffraction, carried out at the MAGS beamline at HZB, gave no indication for a crystallographic/structural anomaly (which would suggest a spin-Peierls transition) down to 1.5 K.
- ²⁶ A.A. Zvyagin, Phys. Lett. A **158**, 333 (1991).